Robert Rantz* and Shad Roundy

Characterization of Real-world Vibration Sources and Application to Nonlinear Vibration Energy Harvesters

DOI 10.1515/ehs-2016-0021

Abstract: A tremendous amount of research has been performed on the design and analysis of vibration energy harvester architectures with the goal of optimizing power output. Often, little attention is given to the actual characteristics of common vibrations from which energy is harvested. In order to shed light on the characteristics of common ambient vibration, data representing 333 vibration signals were downloaded from the NiPS Laboratory "Real Vibration" database, processed, and categorized according to the source of the signal (e. g. vehicle, machine, etc.), the number of dominant frequencies, the nature of the dominant frequencies (e. g. stationary, band-limited noise, etc.), and other metrics. By categorizing signals in this way, the set of idealized vibration inputs (i. e. single stationary frequency, Gaussian white noise, etc.) commonly assumed for harvester input can be corroborated and refined. Furthermore, some heretofore overlooked vibration input types are given motivation for investigation. The classification determined that, of the set of signals used in the study, 64 % of the animal source signals are best described with nonstationary dominant frequencies, 58 % of machine source signals are best described with stationary frequencies, and vehicle source signals are poorly described by any one signal type used in the classification. Nonlinear harvesters with a cubic stiffness term have received extensive attention in the scholarly literature; a numerical simulation and optimization procedure were performed using several representative signals as vibration inputs to determine the prevalence with which such a nonlinear harvester architecture might provide improvement to power output. The analysis indicated that a nonlinear harvester architecture may prove beneficial in increasing power output over a linear counterpart if the signal contains a single, dominant frequency that is not stationary in time, as evidenced by a 14 % increase in harvester power output when employing an architecture with a nonlinear cubic stiffness function. Other studies have indicated that nonlinear architectures may be beneficial for signals with nonstationary frequencies or filtered noise. 53 % of the all characterized signals fall into categories that could potentially benefit from a nonlinear oscillator architecture.

Keywords: energy harvesting, nonlinear harvesters, optimal architectures, vibration classification, vibration database

***Corresponding author: Robert Rantz,** Department of Mechanical Engineering, University of Utah, 1495 E 100 S, Salt Lake City, UT 84112, USA, E-mail: robert.rantz@utah.edu

Shad Roundy, Department of Mechanical Engineering, University of Utah, 1495 E 100 S, Salt Lake City, UT 84112, USA

Introduction

In order to extract sufficient power for a given application, vibration energy harvesters (VEHs) are typically high Q (10-100) resonant oscillators. Thus, their operating bandwidth can be quite narrow. This has motivated an extraordinary amount of research work on methods to increase the operating bandwidth of VEHs (Daqaq et al. 2014; Neiss et al. 2014; Roundy et al. 2005; Wu et al. 2013; Zine-El-Abidine and Yang 2009). Such methods include multi-mode dynamic structures, active frequency tuning by both mechanical and electrical means, and nonlinear dynamic structures. Of course, if the vibration source is dominated by a single stationary frequency, a linear oscillator-based energy harvester is the optimal energy harvesting structure (Halvorsen et al. 2013; Heit and Roundy 2015; Mitcheson et al. 2008; Williams, Woods, and Yates 1996).

In the search for methods to improve the operating bandwidth of VEHs, careful examination and quantification of the types of vibrations that appear frequently in environments conducive to energy harvesting often become a secondary priority; to our knowledge, there has not been a systematic study of the prevalence of vibration sources geared towards determining which VEH structure would be most appropriate for a given source.

The current study seeks to provide additional insight into the prevalence and characteristics of

vibrations commonly encountered in the environment. A broad range of vibrations from the existing NiPS Laboratory "Real Vibration" database is classified using metrics that capture vibration properties that are relevant to VEH design. A comparative analysis of two types of energy harvesting architectures – linear, and nonlinear with a cubic stiffness function – is performed on several representative signals in order to quantify the degree to which a nonlinear architecture could improve power output over a linear architecture, if at all.

Methodology for Classifying Vibrations

The NiPS Laboratory "Real Vibration" database is a library of downloadable vibration signals collected from several types of acquisition kits (Neri et al. 2012). Each signal in the database consists of 3 axes of vibrational data; linear acceleration of X, Y and Z, measured in units of g. Each of the 3 axes is treated as an independent signal for processing purposes. DC bias was removed from each signal axis by subtracting the mean value from the data.

A classification system has been developed for the study that has been previously published (Rantz and Roundy 2016) and is only briefly summarized here.

Signal Sources

The "source" classification of a signal is a broad categorization of what kind of system produced the vibration, as determined by the signal metadata. Source classifications include *Animal, Machine, Vehicle, Structure*, or in the case that the source of the vibration cannot be surmised with confidence, *Unknown*.

Spectrogram Parameters

The entire NiPS database of vibration signals was downloaded and processed into spectrograms for each of the 3 axes, using several sets of processing parameters, generating several spectrograms per vibration signal.

In order to make dominant signals more apparent, a filtering technique was employed based in linear VEH theory. According to the Velocity Damped Resonant Generator (VDRG) model (Mitcheson et al. 2004), the upper bound on average power output of a linear VEH subject to harmonic excitation at resonance is:

$$P_{avg} = \frac{A^2 m \zeta_e}{4\omega(\zeta_m + \zeta_e)^2} \tag{1}$$

where A is the input acceleration amplitude, m is the seismic mass, ζ_m is the mechanical damping ratio, and ζ_e is the electrical damping ratio. (Mitcheson et al. 2004).

Notice that the leading terms A^2 and ω in (1) are properties of the input alone. Determining dominant frequencies is a major component of the classification system presented in this study; thus, in order to make classification more straightforward, spectrograms filtered by only plotting frequency content that is greater than ½ the maximum value of A^2/ω in each FFT frame were plotted alongside unfiltered spectrograms. This filtering process made "dominant" frequencies more distinct, resulting in easier classification of the signal. See Figure 1 for an example spectrogram. Refer to (Rantz and Roundy 2016) for more information on the spectrogram generation procedure and subsequent signal classification.

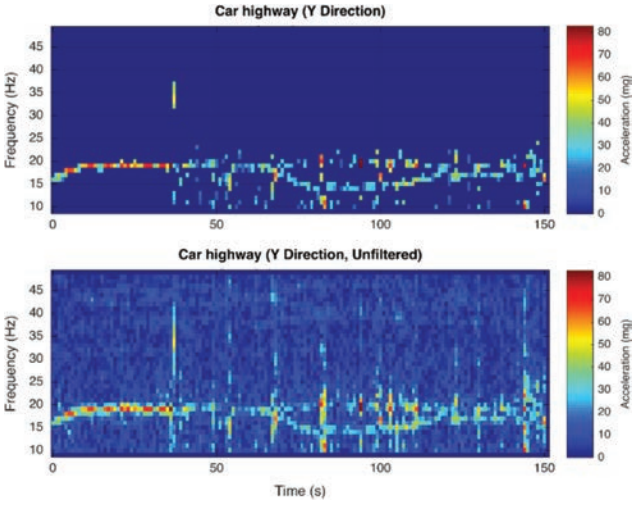

Figure 1: Filtered (top) and unfiltered (bottom) spectrogram used for classification.

Signals with Distinct Dominant Frequencies

Knowledge of the frequencies at which the input power is concentrated has major implications in the design of a VEH architecture, and is therefore of critical importance in any classification scheme intended to shed light on the kinds of vibrations that could be encountered by VEHs.

A *dominant frequency* in the context of this study is a distinct frequency in the signal spectrogram at which the value of A^2/ω is large relative to other frequencies that persists for a substantial duration of the signal.

Vibration signals may have zero, one, or more dominant frequencies. Note that the term *dominant frequency* is derived from the degree to which a particular frequency dominates (in terms of A^2/ω value) a single FFT window, and is thus somewhat of a misnomer; a dominant frequency need not remain at a single frequency throughout the length of the spectrogram.

The time-varying behavior of the dominant frequencies throughout the duration of the signal is also used for classifying the signal. A dominant frequency is considered *stationary* if the frequency at which it occurs does not change much during the length of an input signal. It is possible for some, all, or none of the dominant frequencies of a signal to be stationary.

Signals without Distinct Dominant Frequencies

Many vibration signals do not have distinct, dominant frequencies. Many of these signals can be best described as white noise and filtered noise. For simplicity of classification, two classifiers were employed in this study to describe signals without distinct, dominant frequencies: *White Noise* and *Filtered Noise*.

Amplitude and Noise Tags

Vibrations with inconsistent acceleration amplitudes present unique challenges to nonlinear VEH designs, where both the amplitude and frequency of an input vibration have the capacity to dramatically affect the power output. In order to catalog vibrations with significant swings in amplitude without creating another classification dimension, an *amplitude tag* is applied to all vibrations that change at least (an arbitrarily selected) 50 % over the length of the signal.

Classification Methodology

The entire NiPS database of signals was first downloaded, along with the signal metadata, by virtue of an automated script; at the time of execution, the script downloaded a total of 329 different signals, each with X, Y and Z channels. Spectrograms were then generated for each axis of the signal. The signals, with their associated metadata and spectrograms, were then manually inspected. Signals that did not meet minimum quality criteria were discarded. This process removed 218 signals, leaving 111 left for the study. The classification of each spectrogram was performed manually, by visual inspection of both the spectrogram image file, as well as the (interactive) MATLAB-FIG file.

Vibration Classification Results

Breakdown of Signals by Source

A total of 333 spectrograms were analyzed for the study. A breakdown of all signals by source classification is presented in Figure 2.

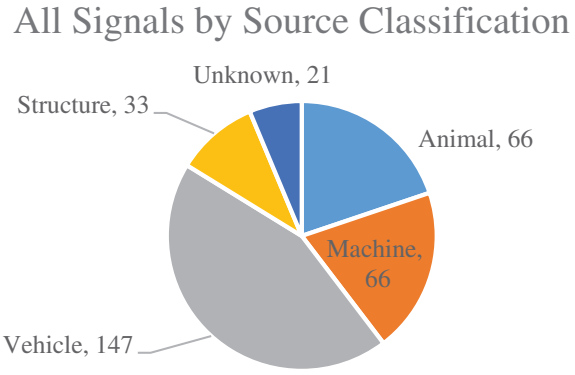

Figure 2: All 333 signals from the study, sorted by source classification.

Breakdown of Signals by Spectrogram Classification

A breakdown of all signals by spectrogram classification is presented in Figure 3.

Most of the signals analyzed in the study can be classified as having a single, dominant frequency. Over a quarter of the total signals can be characterized as lacking a dominant frequency, and are better described by either the White Noise or Filtered Noise categories. A relatively small number of the signals could be classified as having more than one distinct, dominant frequency.

Breakdown of Individual Source Classifications

Perhaps the most important results concern how the signals were characterized for each source. Figure 4 shows the breakdown of characterizations for the Animal sources analyzed in the study.

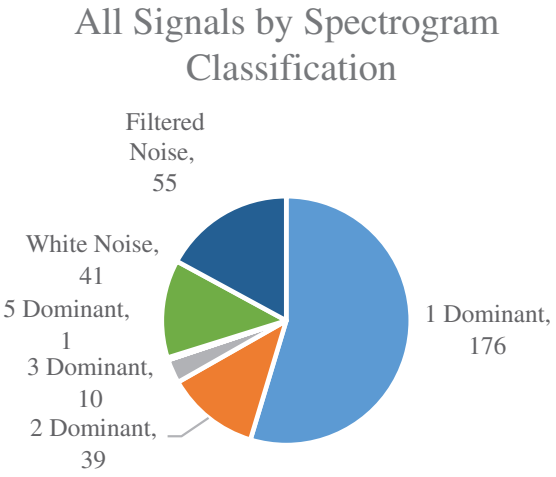

Figure 3: All 333 signals from the study, sorted by spectrogram classification.

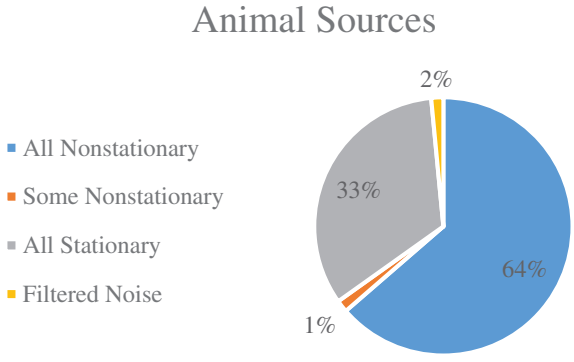

Figure 4: Breakdown of animal sources.

The majority of Animal signals can be described as having dominant frequencies that are nonstationary.

Figure 5 shows the breakdown of characterizations for Machine sources. In this case, the vast majority of signals exhibit either stationary frequencies or are best characterized as noise.

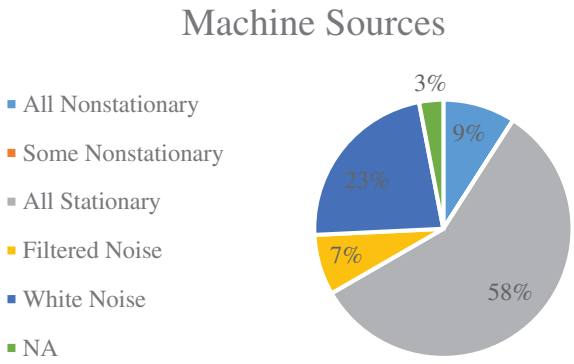

Figure 5: Breakdown of Machine sources.

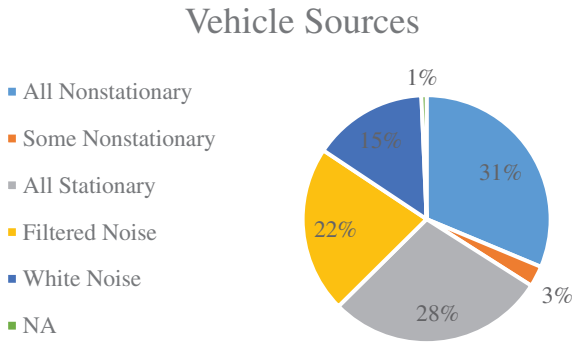

Figure 6: Breakdown of vehicle sources.

Figure 6 shows the breakdown of characterizations for Vehicle sources. Vehicle sources have the most variability in their characterizations; no single category dominates over the others. Dominant frequencies constitute the largest combined category, making up 62% of the classifications. The largest single category is "All Nonstationary," consuming 31% of the total characterizations. This is, perhaps, no surprise; as a vehicle accelerates and decelerates, it is reasonable to assume that the vibrational characteristics will vary with time. "All Stationary" is the second largest category. This may be explained by steady-state vehicle motion; a car moving at constant speed on a highway, for example, may not have any vibrational characteristics that change over the length of the signal.

Figure 7 shows the breakdown of characterizations for Structure sources. For this analysis, a "structure" relates to infrastructure items such as bridges, highways, and buildings. The majority (64%) of the signals derived from Structure sources can best be described as "noisy."

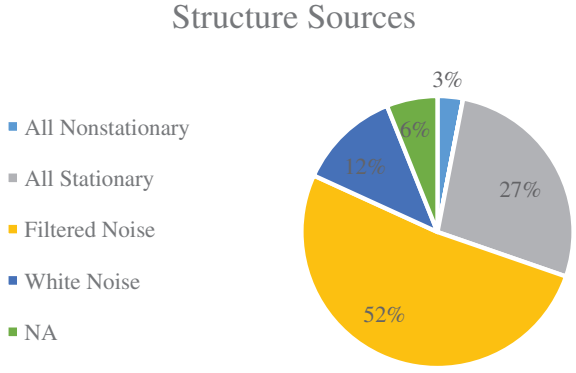

Figure 7: Breakdown of structure sources.

Amplitude Tag

Recall that another important piece of information relevant to VEH design is the time dependence of the vibration amplitude, and that this information is conveyed in this study by virtue of an *amplitude tag*. The amplitude tag can be applied to all classifiable signals; that is, signals not classified as "NA."

Figure 8 displays the frequency with which the amplitude tag was applied to signals, sorted by source classification. It is very clear that time-dependence of vibration amplitude is common in real-world vibration signals, regardless of source.

Method for Comparing Linear and Nonlinear Harvester Architectures

Two vibration energy harvester architectures – one linear, and one with a nonlinear cubic stiffness function – were compared using six representative input signals in order to determine the degree to which the introduction of nonlinearity improves power output, if at all.

The power extracted from the harvester via the electromechanical transducer is assumed to act as an ideal linear damper, as in the VDRG model (Mitcheson et al. 2004). The harvester architectures under consideration may all be described by:

$$m\ddot{z} + (b_m + b_e)\dot{z} + f_s(z) = -\ddot{y} \tag{2}$$

where z is the relative displacement between the base of the harvester and the harvester seismic mass, m is the seismic mass, b_m is the mechanical vicious damping coefficient representing mechanical losses, b_e is the electrical damping coefficient representing the damping imposed by the power transduction mechanism, $f_s(z)$ is the restorative force, and y is the displacement of the base; consequentially, the term y represents the input vibration described by an acceleration signal. A schematic of the system model described by eq. (2) can be found in Figure 9

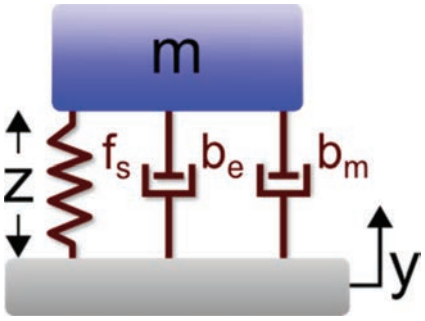

Figure 9: A schematic of the system model described by (2).

In the case of a linear harvester, the restorative force is proportional to displacement:

$$f_s(z) = kz \tag{3}$$

where k is the linear spring constant. Equation (3) in conjunction with eq. (2) represent the VDRG model (Mitcheson et al. 2004). A cubic stiffness function is employed for the nonlinear harvester architecture:

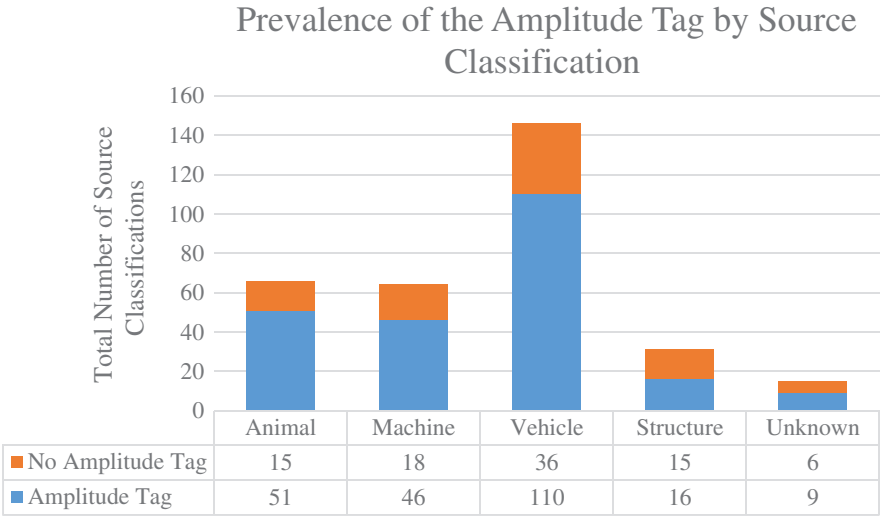

Figure 8: Prevalence of the amplitude tag, broken down by source classification.

$$f_s(z) = \beta z + \alpha z^3 \quad (4)$$

where β is the linear stiffness coefficient, and α is the cubic stiffness coefficient. When the stiffness function described in eq. (4) is substituted into eq. (2), this becomes the familiar Duffing oscillator excited by the input vibration $-y$. When posed in this form, equation eq. (4) conveniently encapsulates a range of qualitatively different nonlinear architectures (Daqaq et al. 2014). If $\beta > 0, \alpha = 0$, then eq. (4) reduces to eq. (3); that is, the restorative force is linear. If $\beta \geq 0, \alpha > 0$ ($\alpha < 0$), the restorative force can be viewed as a hardening (softening) spring. Finally, if $\beta < 0, \alpha > 0$, the resultant system is bistable in nature, characterized by two potential energy wells corresponding to two stable equilibria separated by a potential barrier.

In order to approximate a ceiling on the power that a harvester architecture could achieve, optimization must be performed on the system parameters with the goal of maximizing power dissipation through the electrical damper for a given input signal. The seismic mass, m, and the mechanical damping, b_m. from eq. (2) were considered to be fixed parameters for both linear and nonlinear architectures with values of 1 and 0.02, respectively. The electrical damping, b_e, was an optimization parameter for both architectures.

For the linear architecture exhibiting a stiffness function described by eq. (3), the only additional parameter over which optimization was performed was k, the linear stiffness coefficient. Thus, candidate solutions for the optimization of the linear harvester architecture were two-dimensional, consisting of an electrical damping value, b_e, and a stiffness value, k.

For the nonlinear architecture exhibiting a stiffness function described by eq. (4), two additional optimization parameters were introduced: β, the linear stiffness coefficient, and α the cubic stiffness coefficient. Thus, candidate solutions for the optimization of the nonlinear harvester architecture were three-dimensional, consisting of an electrical damping value, b_e, a linear stiffness coefficient, β, and a cubic stiffness coefficient, α.

An objective function was formed relating the relevant harvester optimization parameters to the power output of the harvester subject to a particular input signal. The relevant design parameters were the input to the objective function; these parameters were used to populate the values in the differential equation that describes the system in eq. (2) and a numerical solver was used to compute the relative motion of the seismic mass in response to the signal input. Having solved for the relative velocity of the mass over the length of the signal T, the power dissipated in the electrical damper was computed via numerical estimation of $P_{avg} = b_e \int_0^T \dot{z}^2 dt$, which was then returned as the output of the solver. The goal of the optimization was to find the design parameters that maximize the harvester output power.

A Pattern Search (PS) algorithm was used in MATLAB (Mathworks 2016) to determine the optimal design parameters for the linear and nonlinear architectures under consideration. Because the objective function requires the numerical solution of eq. (2) subject to fairly long input signals, it was deemed too costly to employ a search method (which may require many function evaluations) in order to inform an initial point for the optimization algorithm. Therefore, in an effort to improve the likelihood that the optimization algorithm converged on or near the global maximum, the algorithm was run multiple times for each signal and each architecture using various initial points, including: a best guess based on the appearance of the spectrogram and, in the case of a linear (nonlinear) architecture, the points near the optimal output for the nonlinear (linear) architecture.

Finally, in order to compare the architectures, the percent change in power from the optimal linear harvester to the optimal nonlinear harvester (found using the PS algorithm) was computed for each representative signal used for the comparison.

Linear and Nonlinear Architecture Comparison Results

Optimal harvester designs were determined using the methodology described in Section 4 and the percent improvement over linear architectures was computed. Approximate values for the percent improvement, as well as values for the optimal β and α, are presented in Table 1.

A linear harvester architecture generally performed as well as the nonlinear harvester architecture in all but one case – Car in highway/X/171 – where the introduction of a nonlinearity in the restorative force resulted in a 14 % improvement of power output over the linear counterpart. As can be seen in Table 1, this single case is also the only significantly nonlinear architecture determined to be optimal by the PS algorithm; in the other cases, the α value (which determines the degree of nonlinearity) is several orders of magnitude lower than the β value,

Table 1: Comparison of optimal linear and nonlinear harvester architectures.

Signal Title/Direction/Number	# Dominant frequencies	Nature	Improvement	Nonlinearity	β [Nm^-1]	α [Nm^-3]
Air Pump/Z/47	2	All Stationary	1 %	Hardening	$77.6 \cdot 10^3$	1.3
Airplane, light turbulence/X/161	>2	0 Stationary	<1 %			
Car in highway/X/171	1	0 Stationary	14 %	Softening	$14.1 \cdot 10^3$	$-99.6 \cdot 10^3$
Chicago metro/Z/165	1	Stochastic	1%	Hardening	$67.7 \cdot 10^3$	1.0
Electric hand shaver/Z/191	1	Stochastic	<1%			
Car highway/Y/229	2	0 Stationary	<1%			

suggesting that the optimal harvester architecture is very nearly linear in these cases.

Discussion

Classifications and Relationship to VEH Design

The study classified a broad range of vibrations from an existing database in order to inform the VEH researcher of the prevalence and characteristics of vibrations seen in real world environments.

The study of 333 signals from the NiPS Real Vibrations database resulted is several interesting conclusions about the available dataset:

The majority of signals do not maintain constant amplitude excitations. This appears to be the case regardless of the source classification.

No single vibration classification appears to describe a single source classification universally. With the exception of the Unknown source classification (not discussed), the greatest portion that any single signal classification consumes within a single source is 64 % (All Nonstationary, Animal). This suggests that proper modelling of a signal from a known source requires more information than simply the source classification of the signal.

Most Animal sources are best described as having distinct dominant frequencies that move with time. 65 % of the signals with the Animal source classification have a dominant component that moved in time. Additionally, nearly half of the Animal signals were embedded in significant levels of noise, as indicated by the number of signals given the noise tag.

Most Machine sources are best described as having distinct dominant frequencies that are stationary, and a substantial portion can best be described using noise. 58 % of the Machine sources analyzed contained dominant frequencies that remained stationary with time, and 9 % contained dominant frequencies that moved with time. 30 % of the Machine sources generated spectrograms that could best be described as "noisy;" that is, 23 % received the "White Noise" classification, and 7 % received the "Filtered Noise" classification.

No single classification dominates the description of Vehicle vibrations. Signals with the Vehicle source classification expressed the most variety in their signal classifications.

Most Structure sources can be described by some type of noise. The White Noise and Filtered Noise signal classifications constitute a combined 64 % of signals that also have the Structure source classification. Nearly all of the remaining signals were classified as having stationary dominant frequencies. Of the signals classified using dominant frequencies, half received the noise tag.

In the case of the single dominant, stationary frequency, it seems unlikely that a novel structure could provide any substantial increase to the maximum power output over a harvester based on a linear oscillator (i. e. characterized by the VDRG model). In fact, it has been shown that for the case of a simple harmonic input, a properly designed linear harvester represents the limiting case of harvester power output (Halvorsen et al. 2013; Heit and Roundy 2015). Of all the signals in the study, approximately 23 % are characterized by a single dominant, stationary frequency.

If the signal can be classified as having multiple dominant, stationary frequencies, then it may be possible to harvest more power from such a signal than could be harvested by a well-designed linear harvester. For example, a multi-mode or wideband harvester might outperform the standard linear oscillator in certain cases. Of all signals in the study, approximately 6 % are characterized by multiple stationary frequencies.

For signals with dominant frequencies that move in time, a tunable harvester would appear to be an appropriate architecture choice, depending on the amount that the frequencies move with time, the characteristic speed with which the frequencies move, and the tuning power

costs of the harvester. Wideband harvester architectures could also provide benefit for this class of signal; harvesters with multiple vibratory modes, for example, or harvesters that employ nonlinear dynamical structures have the potential to provide an increase in power over a linear counterpart with a single resonant peak.

Comparison of Linear and Nonlinear Architectures

Much research has been focused on wideband harvesters exhibiting a nonlinear stiffness function, usually characterized by a cubic stiffness function. Thus, it is worthwhile to investigate how often – in the sample set characterized here – this architecture might provide a significant benefit over a standard linear harvester design. As previously mentioned, such nonlinear harvesters may provide a potential improvement in cases with multiple dominant frequencies or a single moving frequency. Hoffmann (Hoffmann, Folkmer, and Manoli 2012) showed an improvement of 479 % for a test case in which the frequency was linearly swept between a low value and a high value using a monostable nonlinear harvester when compared a linear architecture reference design. The amplitude was held constant for this test case. In the same study, a bi-stable harvester showed very little improvement for multiple stationary frequencies. However, nonlinear harvester architectures represented a significant improvement for an input consisting of band-limited noise. Daqaq (Daqaq 2011) has shown that the shape of the potential function does not affect the power that can be harvested from white noise. Therefore, it is reasonable to conclude that the categories where a significant improvement could be made from a nonlinear harvester are single dominant nonstationary frequency, filtered noise, and multiple dominant stationary frequencies. Taken together, these comprise approximately 53 % of the total signals. It should be noted, however, that such nonlinear structures have a strong amplitude dependence and the majority of signals analyzed have shifting amplitudes. Thus, the real percentage of signals for which a nonlinear design would represent an improvement over a linear design will be somewhat lower.

The comparison of linear and nonlinear harvester architectures described in Section 4 resulted in Table 1 in Section 5. Table 1 suggests that a nonlinear harvester architecture with a cubic stiffness function (softening type, a nonlinear monostable configuration) can improve power output when the input signal can be best described as having a single dominant frequency that moves in time; this conclusion is consistent with results from Hoffmann (Hoffmann, Folkmer, and Manoli 2012). For the particular signal under consideration, however, the power was only 14 % greater than the linear counterpart.

For the other signals described in Table 1, the nonlinear architecture did not appear to significantly improve power output over a linear counterpart; a linear harvester came within 1% of the power output of a nonlinear harvester in all but a single case. This suggests that, in at least these cases, a linear harvester architecture could provide optimal power output.

Limitations of the Study

There are numerous limitations to the study:

Uncertainty in measured data. As previously described, nearly 2/3 of available signals were discarded due to poor quality. Of the signal data that appeared to be useful to the study, the majority were measured using an iPhone as the data acquisition system. This raises several concerns as to the validity of the data; namely, it is unknown if the uploader is qualified to be making careful measurements of the vibration signals, the iPhone sampling rate is limited to 100Hz in the database, there are no specifications regarding the recording conditions (mounting and placement of the iPhone, events that occurred during recording, etc.), the iPhone model used for recording is unknown, and at least one source (Allan 2011) states that the maximum resolution of a particular iPhone accelerometer model is 18 mg. Thus, many of the signals that passed the crude quality check may not be valid representations of the phenomena that was intended for recording.

Subjectivity of analysis. One inescapable consequence of having a human visually examine spectrograms for the purpose of signal classification is the subjectivity of the resulting classifications; although efforts were put in place to prevent obvious misclassification (such as fixing the definition of a particular signal classification before classification began), in many cases, two observers may disagree on the classification of a particular signal. For example, a signal that appears to be characterized by a single dominant frequency embedded in noise to one observer may appear to be better characterized as filtered noise to another observer.

The comparison of linear to nonlinear harvester architectures described in Section 4 also suffers from several limitations that make generalization of the results

difficult. Firstly, the output of the PS optimization algorithm is highly dependent on an initial point as a first iterate (Mathworks 2016). Because of the computational cost of objective function evaluations (which involves numerically solving (2) over lengthy input signals) a search method that could inform the initial point for the PS algorithm (which would likely require many objective function evaluations) was abandoned in exchange for a "best guess" based on the appearance of the signals' spectrograms. Consequentially, it is possible that entire basins of attraction were overlooked by the PS algorithm, and the optimal points at which the algorithm arrived represent locally optimal designs. Furthermore, limits on the accuracy of the numerical solver output, limits on the mesh resolution of the PS algorithm, as well as chaotic motion that could be exhibited by a nonlinear harvester architecture subject to the representative signals used for the comparison, will result in an objective function that is nonsmooth over the solution space; therefore, even if one could guarantee that the initial point for the PS algorithm is placed in the basin of attraction that contains the global optimum, it could not be guaranteed that the PS algorithm could find the global optimum. As a result of these shortcomings, it cannot be stated with certainty that the cases in which a nonlinear harvester architecture *did not* appear to improve power output over a linear counterpart represent cases in which a nonlinear harvester architecture *could not* improve power output over a linear counterpart.

Future work would include a more refined approach in comparing linear and nonlinear VEH architectures. One potential improvement to the proposed method would involve applying a search method to the optimization procedure in order to inform the initial point of the PS algorithm. Such search methods can help to ensure that multiple basins of attraction are considered in the solution space, improving the likelihood that the final output of the PS algorithm is the global optimum.

Conclusions

333 vibration signals from the NiPS Laboratory "Real Vibration" have been characterized and classified by key vibration characteristics. A primary goal of this classification is to provide insight into the design of vibration energy harvesters (VEHs). Determining the prevalence of vibration signals for which standard VEH architectures are optimal is of particular interest. The vibrations were classified by source (i. e. machine, animal, vehicle, structure, unknown). The signals were further characterized by the number of dominant frequencies, whether these frequencies are stationary or move with time, or whether the signal was best characterized by noise, either broadband or filtered. A comparative analysis of linear and nonlinear harvester architectures was performed using six representative signals as inputs. The results of the comparison suggest that a nonlinear harvester architecture exhibiting a cubic stiffness function may offer improvement over a linear counterpart if the input signal can best be described as having a single dominant frequency that moves in time; for the particular signal under consideration, the degree of power improvement was 14 %. However, a linear architecture performed approximately the same for the remaining five representative signals used in the comparative analysis. A qualitative analysis of the set of signals used in the study indicates that a standard linear oscillator harvester is likely the best design for at least 23 % of the signals and that harvesters with the common cubic nonlinear stiffness function could offer an improvement at most 53 % of the time; this is an initial conclusion based on signal classifications and more study is required to refine this result.

Funding: Funding for this research was provided by the National Science Foundation under Award Number ECCS 1342070.

References

Allan, A. 2011. *Basic Sensors in IOS: Programming the Accelerometer, Gyroscope, and More* (illustrate). O'Reilly Media, Inc.

Daqaq, M. F. 2011. "Transduction of a Bistable Inductive Generator Driven by White and Exponentially Correlated Gaussian Noise." *Journal of Sound and Vibration* 330 (11):2554–2564. doi:10.1016/j.jsv.2010.12.005.

Daqaq, M. F., R. Masana, A. Erturk, and D. Dane Quinn. 2014. "On the Role of Nonlinearities in Vibratory Energy Harvesting: A Critical Review and Discussion." *Applied Mechanics Reviews* 66 (4):40801. doi:10.1115/1.4026278.

Halvorsen, E., C. P. Le, P. D. Mitcheson, and E. M. Yeatman. 2013. "Architecture-Independent Power Bound for Vibration Energy Harvesters." *Journal of Physics: Conference Series* 476:117–121. doi:10.1088/1742-6596/476/1/012026.

Heit, J., and S. Roundy. 2015. "A Framework to Find the Upper Bound on Power Output as A Function of Input Vibration Parameters." *Energy Harvesting and Systems* 1–9. doi:10.1115/SMASIS20147444.

Hoffmann, D., B. Folkmer, and Y. Manoli (2012). Comparative Study of Concepts for Increasing the Bandwidth of Vibration Based Energy Harvesters. In *Proceedings of PowerMEMS 2012*, 219–222. http://cap.ee.ic.ac.uk/~pdm97/powermems/2012/oral/O7A-4.pdf

Mathworks. 2016. Global Optimization Toolbox: User's Guide (R2016b). Retrieved September 15, 2016 from http://www.mathworks.com/help/pdf_doc/gads/gads_tb.pdf

Mitcheson, P., T. C. Green, E. M. Yeatman, and A. S. Holmes. 2004. "Architectures For Vibration Driven Micropower Generators." *Journal of Microelectromechanic System* 13 (3):429–440.

Mitcheson, P. D., E. M. Yeatman, G. K. Rao, A. S. Holmes, and T. C. Green. 2008. "Energy Harvesting from Human and Machine Motion for Wireless Electronic Devices." *Proceedings of the IEEE* 96 (9):1457–1486. doi:10.1109/JPROC.2008.927494.

Neiss, S., F. Goldschmidtboeing, M. Kroener, and P. Woias. 2014. Tunable Nonlinear Piezoelectric Vibration Harvester. *Journal of Physics: Conference Series 557*:12113. 10.1088/1742-6596/557/1/012113

Neri, I., F. Travasso, R. Mincigrucci, H. Vocca, F. Orfei, and L. Gammaitoni. 2012. "A Real Vibration Database for Kinetic Energy Harvesting Application." *Journal of Intelligent Material Systems and Structures* 23 (18):2095–2101. doi:10.1177/1045389X12444488.

Rantz, R., and S. Roundy. 2016. "Characterization of Real-World Vibration Sources with a View toward Optimal Energy Harvesting Architectures." *Proceedings SPIE 9801, Industrial and Commercial Applications of Smart Structures Technologies* 9801:98010P. doi:10.1117/12.2219416.

Roundy, S., E. S. Leland, J. Baker, E. Carleton, E. Reilly, E. Lai, B. Otis, J. M. Rabaey, P. K. Wright. V. Sundararajan. 2005. "Improving Power Output for Vibration-Based Energy Scavengers." *IEEE Pervasive Computing* (Jan-March 2005): 28–36. doi:10.1109/MPRV.2005.14.

Williams, C. B., R. C. Woods, and R. B. Yates. 1996. Feasibility Study of a Vibration Powered Micro-Electric Generator. In *Proceedings of IEE Colloquium Conference on Power Sources (Digest No. 96/107)*, 2–4.

Wu, H., L. Tang, Y. Yang, and C. K. Soh. 2013. "A Novel Two-Degrees-Of-Freedom Piezoelectric Energy Harvester." *Journal of Intelligent Material Systems and Structures* 24 (3):357–368. doi:10.1177/1045389X12457254.

Zine-El-Abidine, I., and P. Yang. 2009. "A Tunable Mechanical Resonator." *Journal of Micromechanics and Microengineering* 19 (12):125004. doi:10.1088/0960-1317/19/12/125004.